Hydroxyl Migration in Heterotrimetallic Clusters: An Assessment of Fluxionality Pathways

ARTICLE *in* THE JOURNAL OF PHYSICAL CHEMISTRY A · OCTOBER 2014

Impact Factor: 2.69 · DOI: 10.1021/jp5080835 · Source: PubMed

THE JOURNAL OF PHYSICAL CHEMISTRY A

Article

pubs.acs.org/JPCA

Hydroxyl Migration in Heterotrimetallic Clusters: An Assessment of Fluxionality Pathways

Debashis Adhikari*,†,‡ and Krishnan Raghavachari*,‡

†Department of Chemistry and the Institute of Catalysis for Energy Processes, Northwestern University, Evanston, Illinois 60208, United States

‡Department of Chemistry, Indiana University, Bloomington, Indiana 47405, United States

Supporting Information

ABSTRACT: Water splitting at the unsaturated metal center and subsequent hydroxyl migration are key steps toward successful H_2 liberation from cheap and abundant water using transition metal cluster anions. In this report we initiate a theoretical study (DFT) to assess the efficacy of heterometallic cores instead of the widely studied and well established homometallic cores. To accomplish this goal, one tungsten center in $W_3O_6^-$ core has been replaced by different transition metals such as titanium, technetium, and osmium. Introduction of the heterometal makes the core asymmetric and electronically anisotropic. To evaluate the efficiency of these heterometallic cores, fluxionality pathways for hydroxyl migration have been studied in detail. We show that the cores $W_2TcO_6^-$ (**2**) and $W_2OsO_6^-$ (**3**) can exhibit fluxionality for hydroxyl migration and thus can potentially facilitate H_2 liberation from H_2O. Notably, a new class of low-energy structures generated upon oxide bridge opening process and subsequent structural rearrangement facilitates the hydroxyl migration event. To illustrate the heterometallic effect further, we show that previously inaccessible energy barriers for hydroxyl migration in a homometallic trimolybdenum core become energetically achievable when one of the metals is replaced by a 5d element osmium.

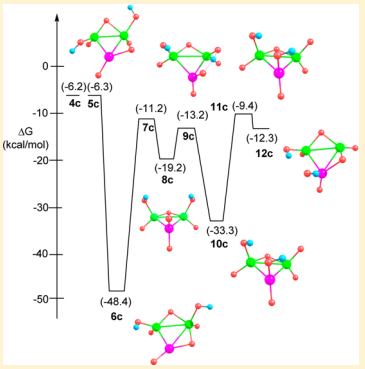

INTRODUCTION

Finding alternative sources of energy to make a sustainable world is a major driving force behind current energy-based research.[1−3] Mimicking natural photosynthesis, capturing and storing the solar energy in a chemical bond (e.g., H_2) is a highly desirable approach to solving the energy problem. The use of H_2 as a fuel is becoming very attractive due to its excellent energy density by mass (143 MJ/kg) and ready availability of the source material such as H_2O,[4] although the splitting of water is a very endothermic process. A significant effort has been invested in designing an economically viable water splitting cell composed of stable semiconductors. In this context, transition metal oxide (TMO) clusters have emerged as promising candidates for liberating H_2 from H_2O and are being actively studied in several groups.[5−10] There is a layer of complexity in the efficiency of TMO clusters since multiple changes can be imagined in terms of the varying nature of the transition metal used, as well as different ligand environments present around the metal centers. In this regard, computational modeling becomes a handy tool to explore active TMO clusters for H_2 liberation from cheap and abundant water. Besides, modeling studies with small TMO clusters can shed light on the mechanism of heterogeneous catalysis on metal surfaces. With that goal in mind, TMO structure and reactivity studies have been pursued by several research groups, using a range of experimental tools in tandem with theoretical methods.[11−25]

Recently Jarrold and co-workers have discovered that group VI metal oxide anions in the gas phase liberate H_2 upon reacting with H_2O.[26−28] A thorough mechanistic investigation has also been conducted to understand many associated details, e.g., to realize that $W_3O_5^-$ core is more efficient in liberating H_2 from water, whereas $Mo_3O_5^-$ core forms a kinetic trap, $Mo_3O_6H_2^-$.[29] All these earlier efforts were performed with homometallic clusters, involving either molybdenum or tungsten. In this work, we compare the activity of heterometallic clusters formed upon changing one of the metals from a homotrimetallic cluster. In previous papers, a distinctly different chemistry has been documented for heterometallic cores compared to their homometallic counterparts. For example, Suzuki and co-workers have noticed that a remarkable acceleration in phosphine/phosphite incorporation and migration of the ligand happens when the core is changed from dinuclear homometallic Cp*Ru(μ-H)$_4$RuCp* (Cp* = pentamethylcyclopentadienyl) to heterometallic Cp*Ru(μ-H)$_4$OsCp*.[30] In another relevant work they also showed a notable and distinct "heterometallic effect" for nitrogen−hydrogen bond cleavage in a trinuclear heterometallic polyhydrido cluster containing ruthenium and osmium.[31,32] As an explanation for the distinguishable heterometallic effect, they propose that introduction of the heterometal atom into a cluster causes structural changes, polarizing the metal−metal bond, and leading to electronic anisotropy. Furthermore,

Received: August 9, 2014
Revised: October 23, 2014

   dx.doi.org/10.1021/jp5080835 | J. Phys. Chem. A XXXX, XXX, XXX−XXX

enhanced Lewis acidity of a particular metal center may be realized as a result of anisotropy that favors nucleophilic attack of substrates. In essence, both the structural change and electronic perturbation upon inclusion of the heterometal directly affect the reactivity of the cluster. In the same vein, Adams and co-workers have shown that mixed metal complexes demonstrate bimetallic cooperativity and synergism in molecular activation that leads to superior activity and better selectivity.[33] To experimentally realize such a heterometallic effect, Domen and co-workers prepared a nanosheet composed of mixed bimetallic $HNbWO_6$ and $HTaWO_6$ aggregates, which are superior solid-acid catalysts for the Friedel−Crafts alkylation of anisole in the presence of benzyl alcohol.[34]

In the context of H_2 liberation from water using TMO clusters, our group has previously shown that an important intermediate responsible for H_2 liberation comprises a metal center having both the hydride and hydroxo functionalities.[17] Such an intermediate can be achieved by fluxionality in a TMO cluster, where a hydroxyl group migrates from one metal center to another. Recently our group has delineated the entire fluxionality pathway for homometallic $Mo_3O_6^-$ and $W_3O_6^-$ cores.[35] Herein our goal is to understand how fluxionality pathway is influenced by a heterometal when it is incorporated in the oxygen deficient $W_3O_6^-$ core by replacing one of the tungsten centers. This report describes a comprehensive computational investigation to understand the effect of heterometal in the $W_2XO_6^-$ core (X = a metal other than tungsten) and is organized into two parts. The first part details the electronic and geometric features of newly designed anionic heterotrimetallic cores and the second part describes the fluxionality pathway as investigated through all these cores to realize the heterometallic effect.

COMPUTATIONAL DETAILS

All calculations have been performed using the B3LYP hybrid density functional.[36,37] The Stuttgart−Dresden (SDD) relativistic pseudopotentials were used to replace the 28, 10, 28, 60, and 60 core electrons of molybdenum, titanium, technetium, tungsten, and osmium, respectively. The remaining valence electrons were treated with a double-ζ basis set augmented with a set of polarization functions of l +1 angular momentum along with a set of diffuse functions needed to describe the extended anionic electron density (s, p, d, and f functions on molybdenum, tungsten, titanium, technetium, and osmium; s, p, and d functions on O). These diffuse and polarization functions were added to the SDD basis set for Mo, W, Ti, Os, and Tc, and the D95 basis set for O. This augmented basis set is denoted as "SDDplus". Optimization of the geometries and vibrational calculations were carried out at the B3LYP/SDDplus level of theory. Open-shell systems were investigated by spin unrestricted formalism and $\langle S^2 \rangle$ values were checked for those optimized geometries to ensure that they depict the correct electronic states. All the minima were confirmed by vibrational calculations without any imaginary frequency. Transition states were characterized by the presence of a single imaginary frequency. Single-point calculations were carried out using augmented triple-ζ quality basis sets at the B3LYP level of theory to get more reliable relative energies. In the triple-ζ quality basis set for the metals, two f-type functions and one g-type function for Mo, W, Ti, Tc, and Os were added to the basis set, as recommended by Martin and Sundermann.[38] The large polarized aug-cc-pVTZ basis set was used for O and H in these calculations. All the relative energies discussed in this article represent the free energies (ΔG) at 298 K. The Gaussian09 program suite has been used for all the calculations.[39]

RESULTS AND DISCUSSION

(a). Structural Aspects of the Heterometallic Cores. Previously, Jarrold and co-workers have probed the structure of the homometallic core $W_3O_6^-$ both experimentally and computationally to reveal that the core is highly symmetric, belonging to C_{3v} point group.[40,41] As expected, the introduction of a heterometal will make the anionic core significantly asymmetric since the terminal and bridging-oxo groups around the heterometal will have different bond lengths compared to the respective bond lengths around the other two metals. In this report we theoretically investigate the type of structural change the anionic tritungsten core undergoes when a heterometal replaces one tungsten and further consider the feasibility of the hydroxyl shuttling pathway, which is conducive to successful production of dihydrogen from water.

Initially we chose Ti as the heterometal since it makes strong oxo-bonds comparable in strength to those involving tungsten (148.8 kcal/mol for Ti═O vs 152.8 kcal/mol for W═O).[42−44] The high metal-oxo bond energy for the group 4 metal has been ascribed to the substantial ionic bonding character.[44] Upon replacement of one tungsten by titanium in a $W_3O_6^-$ core, the resulting $W_2TiO_6^-$ core, **1**, becomes highly asymmetric upon optimization and the molecule belongs to the C_1 symmetry point group. The W(1)−W(2), W(2)−Ti(3), and W(1)−Ti(3) distances in the anionic core are 2.65, 2.72, and 3.04 Å, respectively, which are significantly different from W−W bond lengths in homometallic $W_3O_6^-$ core that exhibits a uniform bond length of 2.62 Å (Figure 1). The terminal tungsten-oxo bond length in anionic core **1** is 1.74 Å, whereas titanium−oxo bond length is 1.64 Å. The ground electronic state of the heterometallic core is a doublet, which is only slightly lower (by 0.01 eV) compared to the excited quartet state. While this is in accordance with our expectation that the lower spin states are more stable as the cluster becomes more and more valence saturated, the energy difference is indeed small. As expected, introduction of Ti inside the anionic core creates asymmetry in charge distribution, and upon closer inspection, Mulliken charges on W(1), W(2), and Ti(3) were found to be 1.15, 1.23, and 0.19e, respectively. The oxygen atom of the terminal titanium oxo group possessed the largest negative charge (Mulliken charge of −0.72e) presumably because of the high electropositive character of titanium. All other terminal and bridged oxo groups are negatively charged in the range of −0.5e. Mulliken spin density analysis discloses that the unpaired spin is completely housed on one of the tungsten centers (for spin density, see S3, Supporting Information). Complete metal centered anionic charge has been observed previously in other TMO clusters.[16]

Since we are interested in studying the hydroxyl migration through different heterometallic anionic cores, we systematically varied the heterometal from early titanium, to late technetium as a 4d transition metal, and then osmium as a 5d transition metal. We chose the heterometal as a representative from each of the 3d, 4d, and 5d series, as well as moving right in the periodic table to pick metals of differing oxo bond strengths. Our chosen cores for this study are $W_2TiO_6^-$ (**1**), $W_2TcO_6^-$ (**2**), and $W_2OsO_6^-$ (**3**), and the logic behind our choice of heterometals has been described later (*vide infra*).

dx.doi.org/10.1021/jp5080835 | J. Phys. Chem. A XXXX, XXX, XXX−XXX

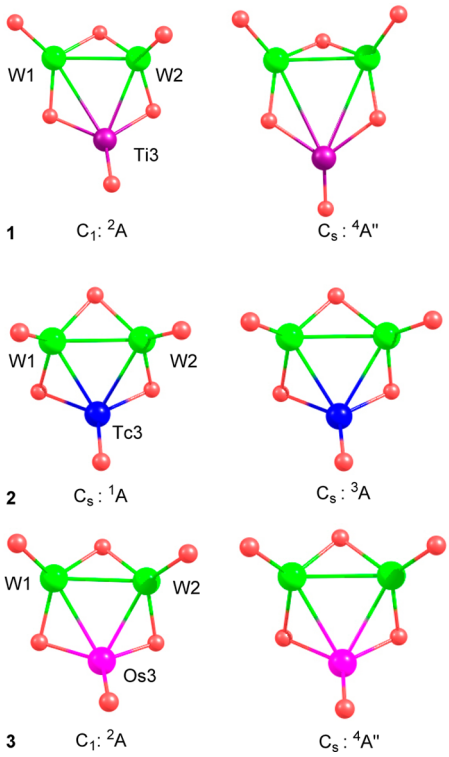

Figure 1. Optimized structures of all the heterometallic oxygen deficient anionic cores considered in this study in both the ground (left column) and excited states (right column). Point group symmetry and important bond lengths are provided. Top line, $W_2TiO_6^-$ (**1**); middle line, $W_2TcO_6^-$ (**2**); bottom line, $W_2OsO_6^-$ (**3**). The connecting line between metals is for illustration purpose only, rather than depiction of a true bond. Color code: green = tungsten; red = oxygen; purple = titanium; blue = technetium; pink = osmium.

The $W_2TcO_6^-$ core (**2**) belongs to the C_s point group and is a ground state singlet, that is only slightly more stable than the excited triplet state (by 0.01 eV). In structure **2**, W−Tc bond lengths (2.54 Å) are very close to the W−W bond length (2.55 Å). This similarity in bond lengths originates from the similar metallic radius of the two metals, tungsten (141 pm) and technetium (135 pm), respectively.[45] For metal−oxo bonds, similarity in bond lengths is again seen since Tc−oxo bond length is observed to be 1.71 Å as compared to W−oxo bond lengths of 1.75 Å. In the excited triplet state of the core **2**, all bonds are significantly elongated, with W−Tc and W−W bond lengths of 2.66 and 2.74 Å, respectively. Overall, the extent of distortion in symmetry for core **2** is significantly less than that in core **1**, presumably because of the similar metallic radii of the metals present in **2**.

The third heterometallic core we considered in this study is $W_2OsO_6^-$ (**3**), which resembles the geometrical features of the core **2**. The ground state of **3** is a doublet, which is more stable than its excited quartet state by 0.02 eV. The core **3** belongs to C_1 point group, and the W−Os bond lengths (2.57 and 2.59 Å) are close to the W−W bond length (2.59 Å). Interestingly, in the excited state geometry, the two W−Os bonds become the same in length (2.73 Å) so that the anionic core retains a C_s symmetry. Terminal W−oxo and Os−oxo bond lengths are essentially the same (1.74 and 1.73 Å, respectively) in the ground state. This is not surprising given the metallic radii of the osmium (1.35 Å) being very close to that of tungsten (1.41 Å).[45] Mulliken charge analysis for core **3** reveals that the charge on tungsten centers is 1.08 and 0.99*e*, whereas the charge on osmium center is 0.19*e*. The unpaired electron is mostly located on tungsten center with a slight amount possessed by the osmium center (0.77 and 0.18*e*, respectively) as inferred through Mulliken spin density analysis. This observation of spin density in the core **3** corroborates well with the spin density distribution we found earlier in core **1**. The frontier molecular orbitals of the studied cores are shown in Figure 2.

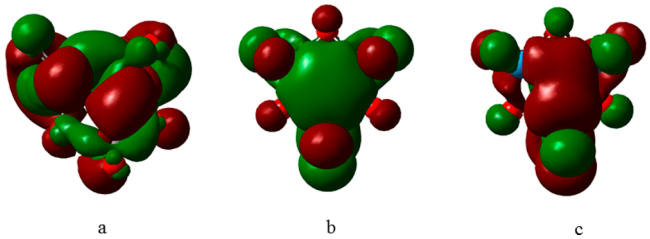

Figure 2. SOMO and HOMO of the three heterometallic cores considered in this study. a, b, c represent the corresponding SOMO of core **1**, HOMO of core **2**, and SOMO of core **3**, respectively.

(b). Feasibility of Hydroxyl Group Migration: Fluxionality Process through the Cores. It has been shown earlier that to carry out H_2 liberation efficiently from water, water needs to be split at a metal center and the resulting hydroxyl group requires migration from one metal center to another to yield hydride and hydroxide ligands on a single metal center.[27,35] Such an intermediate having both the hydride and hydroxyl groups on the same metal center is most amenable to release dihydrogen. It has also been discussed by detailed computational mechanistic analysis that the hydroxyl migration happens actually through proton migration and the interconversion of a terminal oxo ligand to a bridging oxo group.[35]

To evaluate the feasibility of the fluxional nature of the new cores, we started exploring water splitting at W(1) and evaluating the plausibility of hydroxyl migration to the other metal centers in core **1**. W(1) is chosen as the starting center since the Mulliken charge of the center is the highest, so that electrostatic interaction will favor the binding of water. In addition, the products obtained during fluxionality pathways starting at W(1) are thermodynamically more stable than the corresponding products where Ti(3) is the initial water binding site.

The binding of water to W(1) is barrierless and exothermic in nature (by −1.1 kcal mol^{-1}). During formation of the water adduct, two hydrogens of the water are aligned in such a way that weak hydrogen bonding interactions can be attained with the bridging oxo-groups inside the core. Such a stabilizing interaction makes the adduct of water to be thermodynamically slightly downhill. Similar observations regarding the H-bonding interaction favoring the adduct formation have also been recorded earlier.[27,46] We note on passing that a DFT functional such as B3LYP often underestimates the hydrogen bonding strength with respect to MP2 or CCSD(T) results[47] (see details in S1, Supporting Information). Thus, water adduct of anionic core **1** may even be more stable than the result shown above. The splitting of water traverses through a transition state barrier of 3.8 kcal mol^{-1} generating W(1)−oxo and a bridging hydroxyl anchoring W(1) and Ti(3) (Figure 3). This phenomenon results in a slightly asymmetric bridging environment around the metal centers involving the presence of covalent W(1)−OH (2.09 Å) and a Ti(3)−OH bond (2.00 Å).

dx.doi.org/10.1021/jp5080835 | J. Phys. Chem. A XXXX, XXX, XXX−XXX

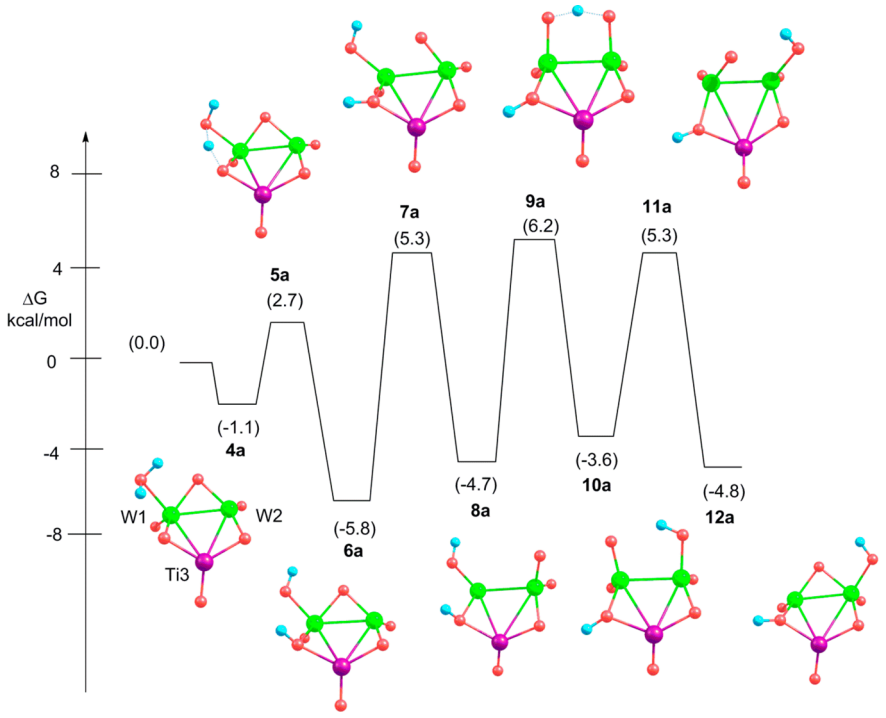

Figure 3. Potential energy (in doublet surface) for water splitting on a tungsten center in core **1** and subsequent migration of hydroxyl group from W(1) to W(2).

The first step for the hydroxyl migration from W(1) center to W(2) is the opening of the oxide-bridge and its subsequent conversion into a terminal oxo-bond at W(2) center.

This preparatory step before hydroxyl migration involving oxide-bridge opening costs a modest energy penalty, 11.1 kcal mol^{-1}, which stems from the loss of W−oxo bond strength at W(1). Overall, the oxide bridge opening generates an intermediate **8a** (Figure 3), which is thermodynamically downhill by 4.7 kcal mol^{-1} compared to the reference state ($W_2TiO_6^-$ core and the water molecule infinitely apart). The proton of the hydroxo group at the W(1) center then migrates to the W(2)−oxo group traversing an energy barrier of 12 kcal mol^{-1}. As expected, the O−H distances at the proton migration transition state (1.21 and 1.25 Å, respectively) are identical to those observed earlier in the homometallic core since the movement involves two tungsten centers.[35] Although it has been reported that many conventional DFT methods over-stabilize structures containing a hydrogen shared between two electronegative atoms, effectively reducing the barrier for proton transfer, B3LYP method is not prone to artificial stabilization and provides a reasonable barrier.[48] Transfer of the proton from the hydroxo group linked to W(1) and W(2) generates an intermediate **10a**, which is slightly thermodynamically downhill, by 3.6 kcal mol^{-1}. The conversion of the terminal W(1)−oxo bond to the bridging oxo-bond between W(1) and W(2) centers is followed with an energy barrier of 11.1 kcal mol^{-1}. Interestingly, the barriers associated with these processes to accomplish hydroxyl migration from W(1) to W(2) center are close in energy and do not suggest a single rate-determining step. These energy barriers remain in the same range as those observed earlier in the homometallic $W_3O_6^-$ core.[35] This fact signifies that the electronic anisotropy generated in the heterometallic core does not strongly influence the hydroxyl migration between two tungsten centers. To test the efficiency of hydroxyl migration through the entire core, ease of hydroxyl migration from W(2) to Ti(3) center needs to be investigated.

After some exploration, in hindsight, we realized that incorporation of a group IV transition metal as the heteroatom is not the best choice due to its inherent inability to do the required valence expansion. Tungsten, a group VI metal, can easily expand its valence to +6, thus the oxo-bridge opening, and other subsequent steps toward the fluxionality pathway, are facilitated in the homometallic $W_3O_6^-$ core. Since titanium cannot support the expansion of valence beyond four, it will arrest the step involving further migration of the hydroxyl group. By a careful computational analysis, we conclude that an alternative pathway for proton migration via the oxide bridge (instead of the mechanism discussed above involving bridge opening and conversion to terminal-oxo) is not feasible due to the high energy involved in the process.

Given the problem of attaining the required valence (preferably +6) by an early transition metal, our next logical choice was to choose a heterometal that can expand its valence to at least six or more. To interrogate further the influence of heterometal in the hydroxyl migration pathway we introduced technetium in the $W_3O_6^-$ core replacing one of the tungsten metals. The reasoning for selecting technetium is to introduce a 4d transition metal, which has the similar metallic radius to tungsten, so that the effect remains largely electronic keeping the geometry distortion to a minimum. The salient geometric features and spin state of the newly designed core **2** has already been described earlier (*vide supra*).

The newly designed anionic core **2** was further tested as a potential candidate for exhibiting fluxionality so that hydroxyl migration can happen from one metal center to the other in the heterometallic core paving the way for H_2 liberation from water. The entire process starts with binding and splitting of water to the W(1) center, followed by migration of the hydroxyl group from W(1) to W(2). As anticipated, the

dx.doi.org/10.1021/jp5080835 | J. Phys. Chem. A XXXX, XXX, XXX−XXX

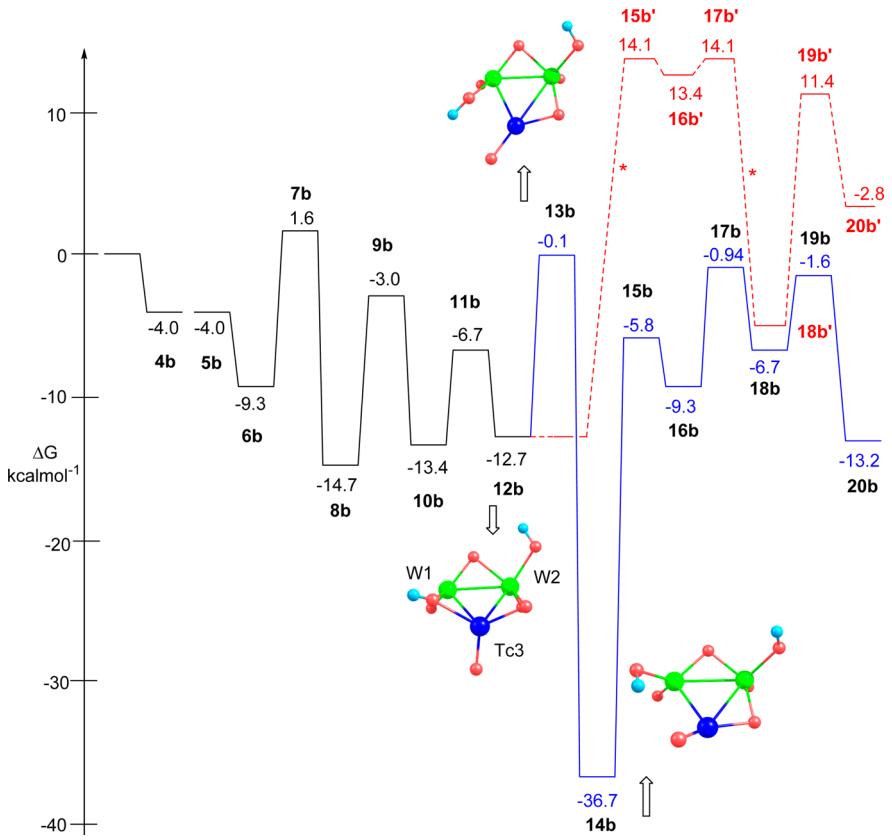

Figure 4. Potential energy surface for two steps of hydroxyl migration pathway in the anionic core **2** is shown. Black trace shows the hydroxyl migration between two tungsten centers, whereas the blue trace shows subsequent migration from W(2) to Tc(3). The red trace in dashed line shows an implausible pathway where a particular family of structures (hydroxo-bridge between W(1) and Tc(3)) is considered (see text). This family of structures with hydroxo-bridge is high in energy and incompatible for hydroxyl shuttling among two metals. The two asterisks on the red trace designate two spin crossovers from singlet to triplet and triplet to singlet state, respectively.

hydroxyl migration between two tungsten centers is minimally affected, with the heterometal technetium behaving as a passive observer (black trace of the PES in Figure 4). All intermediates and transition states (see Figures S1 and S2 for intermediates and transition states, respectively, SI) along this first step of hydroxyl migration exhibit very similar features to those noticed in homometallic core $W_3O_6^-$. In this migration pathway we carefully probed for different spin surfaces and concluded that singlet surface described the lowest energy pathway. The end product of the migration leads to the intermediate structure **12b**, where the migrating hydroxyl group has moved to W(2), and another hydroxyl (generated from water splitting) is bridged between W(1) and Tc(3) (Figure 4).

To accomplish further migration through the core **2**, the hydroxyl group now needs to migrate from W(2) to Tc(3). Following the similar pathway probed previously in our group concerning fluxionality in the homometallic $W_3O_6^-$ core, we notice that the structures en route to hydroxyl migration are high energy species (red trace in the PES diagram, structures **15b′** to **20b′**). So the fluxionality in this part of the core is energetically prohibited, and this will cease the process of complete hydroxyl migration through the core. We note on passing that this high energy pathway involves two spin crossovers. The first happens between **12b** and **15b′** where the pathway moves from singlet to triplet and it reverts back again to singlet between **17b′** and **18b′**. Despite accounting for spin dependence of the structures along the pathway, low energy species remain elusive. To this end we consider whether any other low energy intermediate is accessible from the intermediate **12b**, which can potentially bring down the energy of the subsequent processes. After a thorough search, we observe that opening the hydroxyl bridge between W(1) and Tc(3) generates a new family of structures, which are significantly more stable than the respective hydroxyl-bridge-closed intermediates. The interconversion between these two families of intermediates (**12b** where the OH−bridge is connected to both W(1) and Tc(3) and **14b** where the hydroxyl remains in the open form and is solely connected to W(1)) happens through the TS, **13b** (Figure 4). An important structural change that occurs during this interconversion between intermediates is the switch in orientation of the Tc-oxo bond. This bond orients downward in **12b** (opposite face of hydroxo and the other bridging oxo groups) but becomes upward in **14b**. The TS **13b** for this interconversion truly reflects the gradual change where the hydroxo-bridge opening motion is coupled with the upward movement of the oxo-group attached to technetium. It can be surmised that the structure with the terminal W−OH bond is more stable compared to that of the hydroxo bridge between tungsten and technetium. In addition, this bridge-opening process brings metal centers closer, which is another key factor behind such an enhanced stability for the terminal-hydroxo family of intermediates (*vide infra*). We also note that such a class of intermediates having hydroxyl group in terminal form do not exist during the first hydroxyl migration process between two tungsten centers. This observation is expected since the intermediates having open-

dx.doi.org/10.1021/jp5080835 | J. Phys. Chem. A XXXX, XXX, XXX−XXX

form terminal−OH at W(1) need to possess two terminal hydroxyl groups generating high energy structures. Some of the key transition state structures for implausible red trace versus the accessible blue trace are highlighted in Figure 5.

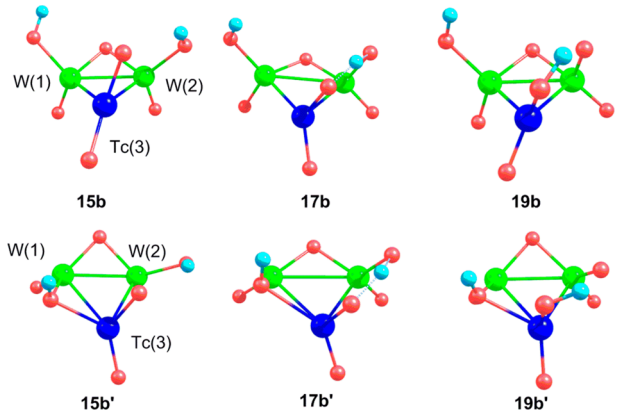

Figure 5. Structural comparison of the key transition states from the energetically feasible pathways (top row) and inaccessible pathways (bottom row). Notice the terminally connected hydroxo group at W(1) in the top row of transition states is bridged between W(1) and Tc(3) in the bottom row of structures.

The second phase of hydroxyl migration, which involves W(2) and Tc(3) happens smoothly for this new family of intermediates as evident from the blue trace in Figure 4. All the species involved in this migration process are significantly more stable than the analogous species in the other family with a hydroxyl group bridging W(1) and Tc(3). The process starts with the oxide-bridge opening, which traverses through an energy barrier of 30.9 kcal mol^{-1}. In this step, a tungsten−oxygen σ-bond is broken while a technetium−oxygen π-bond is formed, yielding intermediate **16b** where the bridged-oxo is converted to terminal-oxo connected solely to technetium. This barrier reflects the strength of the W−oxo bond, as well as the close proximity of W(1) and Tc(3) centers (2.43 Å in **14b** vs 2.54 Å in **16b**). The TS for proton migration is relatively early in nature with the breaking and developing bond lengths of 1.15 and 1.32 Å, respectively. Intermediate **18b** resulting from the proton migration is slightly downhill in energy (−6.7 kcal mol^{-1}), which subsequently traverses through a transition state **19b** to complete the hydroxyl migration step from W(2) to Tc(3). Given the low energy barriers involved for many steps to accomplish fluxionality in the core **2**, it is a highly likely candidate to accomplish liberation of H_2 from H_2O. It is important to notice that the major difference between the red trace and the blue trace (Figure 4) is the structural and stability aspects of intermediates and transition states rather than the nature of individual steps.

Having this promising result described above, we further extended our study to validate the fluxionality pathway in a heterometallic core by choosing another transition metal to make our findings more generally applicable. We introduced a 5d transition metal inside the core and probed the effect of the heterometal in the fluxionality process. Our logic for choosing the heteroatom from 5d row was to introduce greater oxo-bond strength with the heteroatom so that the intermediates formed during the hydroxyl migration event become relatively stable and facilitate the entire pathway. Intuitively, inclusion of 5d metal osmium will make the fluxionality pathway even more facile given the greater bond strength of oxygen to osmium. The primary requirement for valence expansion to six or greater is maintained in our choice for osmium.

In the anionic oxygen deficient core **3**, we primarily focused on the feasibility of the fluxionality pathway involving W(2) and Os(3), with an assumption that the prior splitting of water at W(1) and the migration of the hydroxyl to W(2) remains relatively unperturbed and energetically feasible. At this point, we anticipate that the family of structures having the hydroxyl group terminally connected to W(1) will play a critical role to make the entire migration pathway energetically accessible. The initial binding of water to W(1), its splitting, followed by migration of the hydroxyl group to Os(2) will generate the intermediate **4c** (Figure 6). Intermediate **4c** can convert readily

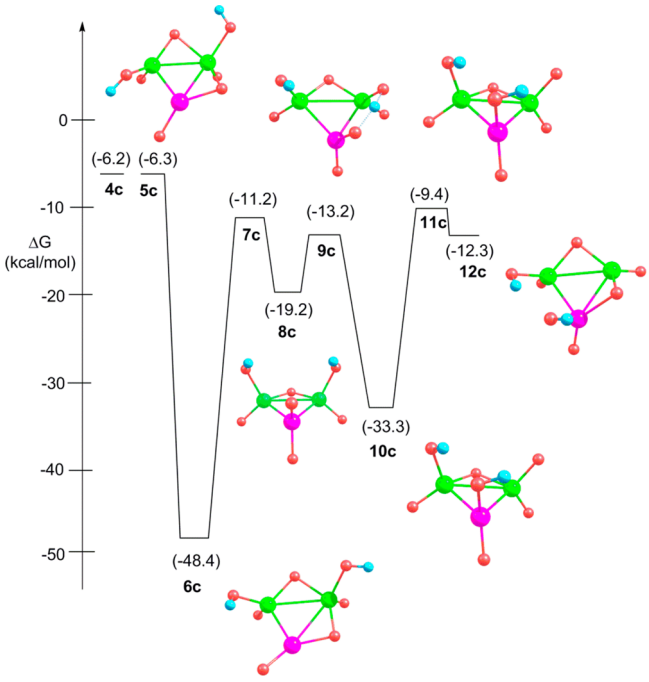

Figure 6. Potential energy surface for hydroxyl migration pathway in core **3** where the migration involves the metal centers tungsten and osmium. Intermediate **4c** is generated after the first hydroxyl migration between two tungsten centers.

into a much stable form of intermediate, **6c** via the TS, **5c**, where both the intermediate and TS are nearly isoenergetic (very low barrier for interconversion). In the intermediate **6c**, the hydroxo functionality is terminally connected to W(1) in its open form that was bridging earlier between W(1) and Os(3) in **4c**. Accordingly, our exploration for the second phase of fluxionality started with intermediate **6c** (Figure 6). As found in the other two cores described above, the pathway starts with the opening of the oxo-bridge between W(2) and Os(3), which has a barrier of 37.2 kcal mol^{-1} followed by the proton migration step traversing through a barrier of 35.2 kcal mol^{-1}. The proton migration TS, **9c** possesses very similar features as observed earlier for the proton migration transition states in core **2**. Further analysis reveals that at the TS the partially broken and partially formed O−H lengths (O−H attached to W(2) is 1.15 Å and the nascent O−H bond linked to Os(3) is 1.34 Å) validate its early nature. The succeeding step to complete the hydroxyl migration includes the interconversion of the terminal Mo−oxo to bridging oxo ligands, which needs

dx.doi.org/10.1021/jp5080835 | J. Phys. Chem. A XXXX, XXX, XXX−XXX

to cross a barrier of 39 kcal mol^{-1}. In this hydroxyl migration pathway, conversion of a terminal-oxo group to bridging-oxo between tungsten and osmium becomes the rate-determining step. In the final product **12c**, the oxo bridge between W(2) and Os(3) is very asymmetric (W(2)−O = 1.87 Å and Os(3)−O = 2.10 Å, respectively), which is expected for two heterometals linking to a bridging oxygen. Overall, the fluxionality pathway between tungsten and osmium is energetically very feasible and substantiates our prior assumption that the introduction of a 5d heterometal will ease the process significantly.

Having seen that inclusion of a heterometal in a trimetallic anionic core can support fluxionality pathways, we probed further to understand the true origin of the heterometallic effect. Upon close scrutiny it appears that in addition to the metal-oxo bond strength of the heterometal, the metal−metal distances play a very important role in this process. Inclusion of a heterometal results in a considerable amount of asymmetry in the core, which triggers a significant rearrangement bringing two metal centers closer. A careful analysis of the structures obtained along the fluxionality pathways reveals these rearranged metal−metal distances and solidifies our argument (Table 1).

Table 1. Comparison of Bond Distance (Å) in Intermediates and Transition States along the Fluxionality Pathway in the Oxygen Deficient Anionic Core 3

structure	W(1)−W(2)	W(1)−Os(3)	W(2)−Os(3)
6c	2.89	2.43	2.87
7c	2.79	2.50	2.67
8c	2.87	2.47	2.47
9c	2.92	2.50	2.48
10c	2.96	2.39	2.54
11c	2.78	2.47	2.59
12c	2.81	2.43	2.56

As seen from Table 1, the distance between two tungsten centers in all the intermediates and transition states are slightly longer than the metal−metal distance in the bulk (2.74 Å).[49,50] In comparison, W(1)−Os(3) distance in those structures are significantly shorter indicating a higher bond order than 1 for these bonds. The proximity of the metal centers W(1) and Os(3) is a result of the rearrangement where the hydroxyl group is terminally attached to W(1) center rather than acting as a bridge. As an example, W(1)−Os(3) bond in the core **3** (2.73 Å) is changed to 2.39 Å in the intermediate **10c** while displaying fluxionality. As a further proof, a very similar trend is noticed in the case of core **2**, where W(1)−Tc(3) distance in the parent core **2** (2.54 Å) is changed to 2.36 Å in the intermediate **18b**. This close proximity of two metal centers resulting from the rearrangement significantly enhances the metal−metal bond strength, thus stabilizing structures related to the fluxionality process. This is also in accordance with Dixon's observation: multicenter metal−metal bonding is a common feature for second and third row TMO clusters, partly due to the strong relativistic effects associated with the third row transition metals, leading to more diffuse d orbitals and stronger metal−metal interactions.[44]

Through this investigation we proved that heterometallic cores can be a viable option for exhibiting fluxionality and can behave as a potential candidate toward successful H_2 liberation from H_2O. Realizing this heterometallic effect, we hypothesized whether such an effect can even make an "incompetent" homometallic core to become fluxionally "competent". To investigate this, we chose the homometallic $Mo_3O_6^-$ core, which did not display fluxionality, due to the presence of higher energy barriers as found in our previous investigation.[35] Herein, we want to introduce a heterometal in this $Mo_3O_6^-$ core replacing one of the molybdenums and test whether the resulting core can demonstrate fluxionality. Accordingly, we introduced osmium as the heterometal in the core given the most prominent heterometallic rearrangement exhibited by the metal in core **3**. The second phase of hydroxyl migration between Mo(2) and Os(3) centers is described in Figure 7. As

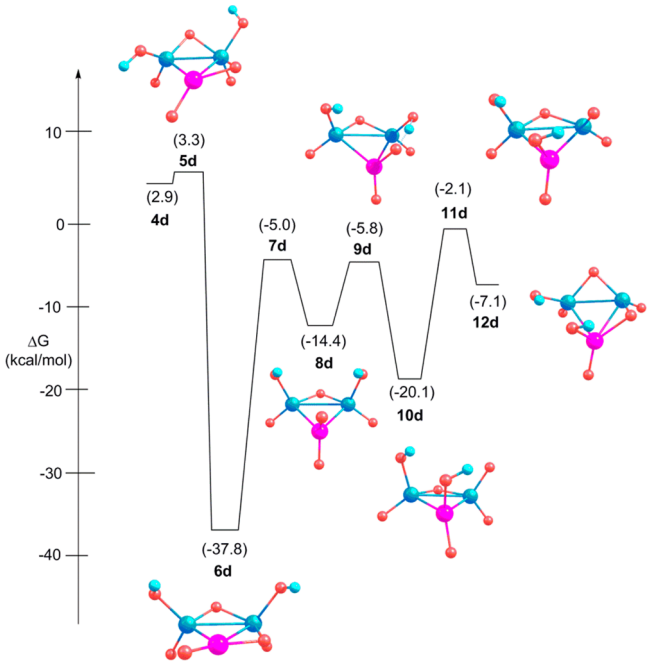

Figure 7. Potential energy surface for hydroxyl migration pathway in $Mo_2OsO_6^-$ core after water splitting at Mo(1). The hydroxyl group migrates from the second molybdenum to osmium center. The intermediate **4d** is generated via the first hydroxyl migration between two molybdenum centers.

depicted in the potential energy surface, all the steps associated with the fluxional behavior remain energetically accessible and should take place under experimental conditions. In accordance with our earlier findings, a new class of low-energy structures (e.g., **6d**) is obtained upon opening the hydroxo-bridge between Mo(1) and Os(3). The TS connecting the hydroxo-bridge structures and hydroxo-terminal structures is only 3.3 kcal mol^{-1} high in energy. Upon rearrangement, the resulting structure **6d** becomes very stable (−37.8 kcal mol^{-1}), and it follows the regular sequence of steps to accomplish fluxionality. In the structure **6d**, the Mo(1)−Os(3) distance (2.42 Å) is short and describes significant metal−metal bonding. This phenomenon of rearrangement in the core, bringing two metal centers into close proximity, stabilizes the intermediates along the fluxionality pathway and strengthens our conclusion that the inclusion of a proper heterometal (late 4d and 5d transition metals) can make the fluxionality process very facile.

CONCLUSIONS

In this study we have investigated oxygen deficient anionic cores consisting of a trinuclear heterometallic system. Previous

dx.doi.org/10.1021/jp5080835 | J. Phys. Chem. A XXXX, XXX, XXX−XXX

studies involving H_2 liberation from water by the anionic cores focused only on homometallic systems. In this present study, we incorporate a heterometal that makes the structure geometrically asymmetric, resulting in inhomogeneous electron distribution throughout the core. Investigations of fluxionality pathways through these newly furnished cores help us draw some important conclusions. The hydroxyl migration between the same metals such as two tungsten centers is largely unaffected even in heterometallic cores. However, fluxionality through the entire core requires subsequent migration of the hydroxyl group from tungsten to the heterometal, which becomes energetically very feasible when 4d and 5d metals are used as a heterometal. The hydroxyl migration between two heterometals becomes energetically very accessible when a family of structures having hydroxyl group connected to only W(1) was considered. Among the choice of heterometals, a 5d metal shows the best performance in bringing the energy of the intermediates and transition states down and making the fluxionality pathway highly feasible. The rearrangement facilitated by the inclusion of the heterometal enhances the metal−metal interactions and bond strengths and lowers the energy of the new family of structures. Incorporation of the heterometal provides valuable insights in designing new anionic metal cores that can be effective in releasing H_2 from cheap and abundant H_2O.

■ ASSOCIATED CONTENT

Supporting Information

Spin density plot, $\langle S^2 \rangle$ values for spin unrestricted calculations, structure of intermediates, and Cartesian coordinates of all the investigated structures. This material is available free of charge via the Internet at http://pubs.acs.org.

■ AUTHOR INFORMATION

Corresponding Authors

*E-mail: d-adhikari@northwestern.edu.

*E-mail: kraghava@indiana.edu.

Notes

The authors declare no competing financial interest.

■ ACKNOWLEDGMENTS

This work was entirely supported by Department of Energy Grant No. DE-FG02-07ER15889 at Indiana University. D.A. gratefully acknowledges the generous financial support from Northwestern University.

■ REFERENCES

(1) Nocera, D. G. Living Healthy on a Dying Planet. *Chem. Soc. Rev.* **2009**, *38*, 13−15.

(2) Lewis, N. S.; Nocera, D. G. Powering the Planet: Chemical Challenges in Solar Energy Utilization. *Proc. Natl. Acad. Sci. U.S.A.* **2006**, *103*, 15729−15735.

(3) Whitesides, G. M.; Crabtree, G. W. Don't Forget Long-Term Fundamental Research in Energy. *Science* **2007**, *315*, 796−798.

(4) Cook, T. R.; Dogutan, D. K.; Reece, S. Y.; Surendranath, Y.; Teets, T. S.; Nocera, D. G. Solar Energy Supply and Storage for the Legacy and Nonlegacy Worlds. *Chem. Rev.* **2010**, *110*, 6474−6502.

(5) Maeda, K.; Teramura, K.; Lu, D.; Takata, T.; Saito, N.; Inoue, Y.; Domen, K. Photocatalyst Releasing Hydrogen From Water. *Nature* **2006**, *440*, 295−295.

(6) Maeda, K.; Teramura, K.; Lu, D.; Saito, N.; Inoue, Y.; Domen, K. Noble-Metal/Cr_2O_3 Core/Shell Nanoparticles as a Cocatalyst for Photocatalytic Overall Water Splitting. *Angew. Chem., Int. Ed.* **2006**, *45*, 7806−7809.

(7) Yoshida, M.; Takanabe, K.; Maeda, K.; Ishikawa, A.; Kubota, J.; Sakata, Y.; Ikezawa, Y.; Domen, K. Role and Function of Noble-Metal/Cr-Layer Core/Shell Structure Cocatalysts for Photocatalytic Overall Water Splitting Studied by Model Electrodes. *J. Phys. Chem. C* **2009**, *113*, 10151−10157.

(8) Yoshida, M.; Maeda, K.; Lu, D.; Kubota, J.; Domen, K. Lanthanoid Oxide Layers on Rhodium-Loaded $(Ga_{1-x}Zn_x)(N_{1-x}O_x)$ Photocatalyst as a Modifier for Overall Water Splitting under Visible-Light Irradiation. *J. Phys. Chem. C* **2013**, *117*, 14000−14006.

(9) Maeda, K.; Domen, K. Photocatalytic Water Splitting: Recent Progress and Future Challenges. *J. Phys. Chem. Lett.* **2010**, *1*, 2655−2661.

(10) Sakamoto, N.; Ohtsuka, H.; Ikeda, T.; Maeda, K.; Lu, D.; Kanehara, M.; Teramura, K.; Teranishi, T.; Domen, K. Highly Dispersed Noble-Metal/Chromia (Core/Shell) Nanoparticles as Efficient Hydrogen Evolution Promoters for Photocatalytic Overall Water Splitting under Visible Light. *Nanoscale* **2009**, *1*, 106−109.

(11) Pramann, A.; Koyasu, K.; Nakajima, A.; Kaya, K. Photoelectron Spectroscopy of Cobalt Oxide Cluster Anions. *J. Phys. Chem. A* **2002**, *106*, 4891−4896.

(12) Gong, Y.; Zhou, M.; Andrews, L. Spectroscopic and Theoretical Studies of Transition Metal Oxides and Dioxygen Complexes. *Chem. Rev.* **2009**, *109*, 6765−6808.

(13) Wu, H.; Desai, S. R.; Wang, L.-S. Chemical Bonding between Cu and Oxygen−Copper Oxides vs O_2 Complexes: A Study of CuO_x (x = 0−6) Species by Anion Photoelectron Spectroscopy. *J. Phys. Chem. A* **1997**, *101*, 2103−2111.

(14) Gutsev, G. L.; Weatherford, C. A.; Pradhan, K.; Jena, P. Structure and Spectroscopic Properties of Iron Oxides with the High Content of Oxygen: FeO_n and FeO_n^- (n = 5−12). *J. Phys. Chem. A* **2010**, *114*, 9014−9021.

(15) Sun, Q.; Rao, B. K.; Jena, P.; Stolcic, D.; Ganteför, G.; Kawazoe, Y. Effect of Sequential Oxidation on the Electronic Structure of Tungsten Clusters. *Chem. Phys. Lett.* **2004**, *387*, 29−34.

(16) Zhai, H.-J.; Huang, X.; Cui, L.-F.; Li, X.; Li, J.; Wang, L.-S. Electronic and Structural Evolution and Chemical Bonding in Ditungsten Oxide Clusters: $W_2O_n^-$ and W_2O_n (n = 1−6). *J. Phys. Chem. A* **2005**, *109*, 6019−6030.

(17) Zhai, H.-J.; Kiran, B.; Cui, L.-F.; Li, X.; Dixon, D. A.; Wang, L.-S. Electronic Structure and Chemical Bonding in MO_n^- and MO_n Clusters (M = Mo, W; n = 3−5): A Photoelectron Spectroscopy and Ab Initio Study. *J. Am. Chem. Soc.* **2004**, *126*, 16134−16141.

(18) Sun, Q.; Rao, B. K.; Jena, P.; Stolcic, D.; Kim, Y. D.; Gantefor, G.; Castleman, A. W. Appearance of Bulk Properties in Small Tungsten Oxide Clusters. *J. Chem. Phys.* **2004**, *121*, 9417−9422.

(19) Mayhall, N. J.; Rothgeb, D. W.; Hossain, E.; Raghavachari, K.; Jarrold, C. C. Electronic Structures of $MoWO_y^-$ and $MoWO_y$ Determined by Anion Photoelectron Spectroscopy and DFT Calculations. *J. Chem. Phys.* **2009**, *130*, 124313.

(20) Li, S.; Dixon, D. A. Molecular and Electronic Structures, Brönsted Basicities, and Lewis Acidities of Group VIB Transition Metal Oxide Clusters. *J. Phys. Chem. A* **2006**, *110*, 6231−6244.

(21) Li, S.; Dixon, D. A. Low-Lying Electronic States of $M_3O_9^-$ and $M_3O_9^{2-}$ (M = Mo, W). *J. Phys. Chem. A* **2007**, *111*, 11093−11099.

(22) Li, S.; Hennigan, J. M.; Dixon, D. A.; Peterson, K. A. Accurate Thermochemistry for Transition Metal Oxide Clusters. *J. Phys. Chem. A* **2009**, *113*, 7861−7877.

(23) Li, S.; Dixon, D. A. Benchmark Calculations on the Electron Detachment Energies of MO_3^- and $M_2O_6^-$ (M = Cr, Mo, W). *J. Phys. Chem. A* **2007**, *111*, 11908−11921.

(24) Zhai, H.-J.; Li, S.; Dixon, D. A.; Wang, L.-S. Probing the Electronic and Structural Properties of Chromium Oxide Clusters $(CrO_3)^{n-}$ and $(CrO_3)^n$ (n = 1−5): Photoelectron Spectroscopy and Density Functional Calculations. *J. Am. Chem. Soc.* **2008**, *130*, 5167−5177.

(25) Bertram, N.; Kim, Y. D.; Ganteför, G.; Sun, Q.; Jena, P.; Tamuliene, J.; Seifert, G. Experimental and Theoretical Studies on Inorganic Magic Clusters: M_4X_6 (M = W, Mo; X = O, S). *Chem. Phys. Lett.* **2004**, *396*, 341−345.

(26) Rothgeb, D. W.; Hossain, E.; Kuo, A. T.; Troyer, J. L.; Jarrold, C. C.; Mayhall, N. J.; Raghavachari, K. Unusual Products Observed in Gas-Phase $W_xO_y^-$ + H_2O and D_2O Reactions. *J. Chem. Phys.* **2009**, *130*, 124314.
(27) Mayhall, N. J.; Rothgeb, D. W.; Hossain, E.; Jarrold, C. C.; Raghavachari, K. Water Reactivity with Tungsten Oxides: H_2 Production and Kinetic Traps. *J. Chem. Phys.* **2009**, *131*, 144302.
(28) Rothgeb, D. W.; Hossain, E.; Mayhall, N. J.; Raghavachari, K.; Jarrold, C. C. Termination of the $W_2O_y^-$ + $H_2O/D_2O \rightarrow W_2O_{y+1}^-$ + H_2/D_2 Sequential Oxidation Reaction: An Exploration of Kinetic versus Thermodynamic Effects. *J. Chem. Phys.* **2009**, *131*, 144306.
(29) Ramabhadran, R. O.; Mann, J. E.; Waller, S. E.; Rothgeb, D. W.; Jarrold, C. C.; Raghavachari, K. New Insights on Photocatalytic H_2 Liberation from Water Using Transition-Metal Oxides: Lessons from Cluster Models of Molybdenum and Tungsten Oxides. *J. Am. Chem. Soc.* **2013**, *135*, 17039−17051.
(30) Kameo, H.; Nakajima, Y.; Suzuki, H. Drastic Acceleration of Phosphine/Phosphite Incorporation into a Tetrahydrido Ruthenium/Osmium Complex, and One-way Ruthenium to Osmium Migration of a Phosphorus Ligand. *Angew. Chem., Int. Ed.* **2008**, *47*, 10159−10162.
(31) Kameo, H.; Nakajima, Y.; Namura, K.; Suzuki, H. Heterometallic Effects in Nitrogen−Hydrogen Bond Cleavage by Trinuclear Mixed-Metal Polyhydrido Clusters Containing Ruthenium and Osmium. *Organometallics* **2011**, *30*, 6703−6712.
(32) Kameo, H.; Shima, T.; Nakajima, Y.; Suzuki, H. Synthesis of Heterometallic Trinuclear Polyhydrido Clusters Containing Ruthenium and Osmium and Their Electronic and Structural Deviation from Homometallic Systems. *Organometallics* **2009**, *28*, 2535−2545.
(33) Adams, R. D.; Captain, B. Unusual Structures and Reactivity of Mixed Metal Cluster Complexes Containing the Palladium/Platinum Tri-t-butylphosphine Grouping. *Acc. Chem. Res.* **2009**, *42*, 409−418.
(34) Tagusagawa, C.; Takagaki, A.; Hayashi, S.; Domen, K. Characterization of $HNbWO_6$ and $HTaWO_6$ Metal Oxide Nanosheet Aggregates As Solid Acid Catalysts. *J. Phys. Chem. C* **2009**, *113*, 7831−7837.
(35) Ramabhadran, R. O.; Mayhall, N. J.; Raghavachari, K. Proton Hop Paving the Way for Hydroxyl Migration: Theoretical Elucidation of Fluxionality in Transition-Metal Oxide Clusters. *J. Phys. Chem. Lett.* **2010**, *1*, 3066−3071.
(36) Becke, A. D. Density-Functional Thermochemistry. III. The Role of Exact Exchange. *J. Chem. Phys.* **1993**, *98*, 5648−5652.
(37) Lee, C.; Yang, W.; Parr, R. G. Development of the Colle-Salvetti Correlation-Energy Formula into a Functional of the Electron Density. *Phys. Rev. B* **1988**, *37*, 785−789.
(38) Martin, J. M. L.; Sundermann, A. Correlation Consistent Valence Basis Sets for Use with the Stuttgart−Dresden−Bonn Relativistic Effective Core Potentials: The Atoms Ga−Kr and In−Xe. *J. Chem. Phys.* **2001**, *114*, 3408−3420.
(39) Frisch, M. J.; Trucks, G. W.; Schlegel, H. B.; Scuseria, G. E.; Robb, M. A.; Cheeseman, J. R.; Scalmani, G.; Barone, V.; Mennucci, B.; Petersson, G. A.; et al. *Gaussian 09*, revision A.02; Gaussian Inc.: Wallingford, CT, 2009.
(40) Rothgeb, D. W.; Mann, J. E.; Waller, S. E.; Jarrold, C. C. Structures of Trimetallic Molybdenum and Tungsten Suboxide Cluster Anions. *J. Chem. Phys.* **2011**, *135*, 104312.
(41) Rothgeb, D. W.; Hossain, E.; Mann, J. E.; Jarrold, C. C. Disparate Product Distributions Observed in $Mo_{(3-x)}W_xO_y^-$(x = 0−3; y = 3−9) Reactions with D_2O and CO_2. *J. Chem. Phys.* **2010**, *132*, 064302.
(42) Carter, E. A.; Goddard, W. A. Early- versus Late-Transition-Metal-Oxo Bonds: The Electronic Structure of Oxovanadium(1+) and Oxoruthenium(1+). *J. Phys. Chem.* **1988**, *92*, 2109−2115.
(43) Mayhall, N. J.; Becher, E. L., III; Chowdhury, A.; Raghavachari, K. Molybdenum Oxides versus Molybdenum Sulfides: Geometric and Electronic Structures of $Mo_3X_y^-$ (X = O, S and y = 6, 9) Clusters. *J. Phys. Chem. A* **2011**, *115*, 2291−2296.
(44) Li, S.; Dixon, D. A. In *New and Future Developments in Catalysis*; Suib, S. L., Ed.; Elsevier: Amsterdam, The Netherlands, 2013; pp 21−61.
(45) Li, W.-K.; Zhou, G.-D.; Mak, T. C. W. *Advanced Structural Inorganic Chemistry*; Oxford University Press: New York, 2008.
(46) Saha, A.; Raghavachari, K. Hydrogen Evolution from Water through Metal Sulfide Reactions. *J. Chem. Phys.* **2013**, *139*, 204301−204312.
(47) Ireta, J.; Neugebauer, J.; Scheffler, M. On the Accuracy of DFT for Describing Hydrogen Bonds: Dependence on the Bond Directionality. *J. Phys. Chem. A* **2004**, *108*, 5692−5698.
(48) Barone, V.; Adamo, C. Proton Transfer in the Ground and Lowest Excited States of Malonaldehyde: A Comparative Density Functional and Post-Hartree-Fock Study. *J. Chem. Phys.* **1996**, *105*, 11007−11019.
(49) Bino, A.; Cotton, F. A.; Dori, Z.; Sekutowski, J. C. Preparation and Characterization of Di-.Mu.-Sulfido Binuclear Compounds of Tungsten(IV) and -(V). Unambiguous Examples of Formal Single and Double Bonds Between Tungsten Atoms. *Inorg. Chem.* **1978**, *17*, 2946−2950.
(50) Abrahamson, H. B.; Heeg, M. J. Hexacarbonyl(fulvalene)-ditungsten(W-W). A Stretched Tungsten-Tungsten Single Bond. *Inorg. Chem.* **1984**, *23*, 2281−2286.